Lipid phase behaviour under steady state conditions

Christoffer Åberg,[ab] Emma Sparr[a] and Håkan Wennerström*[a]

Received 22nd April 2012, Accepted 1st June 2012
DOI: 10.1039/c2fd20079a

At the interface between two regions, for example the air–liquid interface of a lipid solution, there can arise non-equilibrium situations. The water chemical potential corresponding to the ambient RH will, in general, not match the water chemical potential of the solution, and the gradients in chemical potential cause diffusional flows. If the bulk water chemical potential is close to a phase transition, there is the possibility of forming an interfacial phase with structures qualitatively different from those found in the bulk. Based on a previous analysis of this phenomenon in two component systems (C. Åberg, E. Sparr, K. Edler and H. Wennerström, *Langmuir*, 2009, **25**, 12177), we here analyse the phenomenon for three-component systems. The relevant transport equations are derived, and explicit results are given for some limiting cases. Then the formalism is applied conceptually to four different aqueous lipid systems, which in addition to water and a phospholipid contain (i) octyl glucoside, (ii) urea, (iii) heavy water, and (iv) sodium cholate as the third component. These four cases are chosen to illustrate (i) a method to use a micelle former to transport lipid to the interface where a multi-lamellar structure can form; (ii) to use a co-solvent to inhibit the formation of a gel phase at the interface; (iii) a method to form pure phospholipid multi-lamellar structures at the interface; (iv) a method to form a sequence of phases in the interfacial region. These four cases all have the character of theoretically based conjectures and it remains to investigate experimentally whether or not the conditions can be realized in practice.

1. Introduction

The living system is highly dynamic. It is an old debate whether or not the study of equilibrium properties can shed light on what is going on in the living cell. The huge success of molecular biology during the last sixty years has to a substantial degree been based on studies of equilibrium systems, clearly demonstrating that such investigations are relevant. However, it is equally obvious that in order to get a more complete understanding it is necessary to go beyond the equilibrium picture and analyse also dynamics and transport processes. The primary aspects of the dynamics are the chemical transformation of metabolites from their initial form to end products, and the regulation of the complex machineries that accomplish such transformations. Currently, studies of such intricate couplings are characterized by the term systems biology. In the present paper we address another aspect of the dynamics. The general question we pose is: does the fact that one has non-equilibrium

[a]*Division of Physical Chemistry, Chemical Center, Lund University, P.O.Box 124, SE-22100 Lund, Sweden. E-mail: hakan.wennerstrom@fkem1.lu.se; emma.sparr@fkem1.lu.se; Fax: +46 46 2224413*
[b]*Centre for BioNano Interactions, School of Chemistry and Chemical Biology, University College Dublin, Belfield, Dublin 4, Ireland. E-mail: christoffer.aberg@cbni.ucd.ie*

transport processes in the system affect structural properties and, in particular, to what extent does it affect lipid phase behaviour?

One major role of lipid structures in the living cell is to separate regions with different properties, as, for example, the intra- and extracellular regions. It is clear that the thermodynamic conditions can be different on the two sides of the barrier membrane. Since lipids can adopt a range of structures one can have the situation that for values of the thermodynamic parameters on one side of the lipid barrier, the lipids prefer one structural arrangement, while for the conditions on the other side, another structure is the preferred one. Such a scenario is an obvious possibility across the (human) skin[1,2] and across the membrane system in the alveoli of the lung,[3] but there are potentially many more situations where one could consider the possibility of such complications.

In laboratory studies of lipid systems, one also needs to be aware of the possibility of non-equilibrium effects. In a typical Langmuir trough laboratory setup there is not full control of the thermodynamic conditions of the gas phase. It is the rule rather than the exception that the relative humidity (RH) of the gas phase does not match the chemical potential of the water ($\mu(H_2O)$) in the liquid phase. This generates non-equilibrium transport processes across the air–water interface, which could in turn give rise to unexpected structural changes. Similar conditions exist also in the lipid tear film formed on our eyes, which indeed should act to prevent evaporation and dry eyes.[9]

In a recent publication[10] we analysed possibilities of forming lamellar structures triggered by transport processes at the air–water interface. We analysed the general two component water–amphiphile case and applied it to the specific AOT (bis(2-ethylhexyl)sulfosuccinate)–water system. In this case we could base the quantitative analysis on a previous thorough equilibrium characterization of the bulk system.[11,12] We showed that a multilamellar structure could form at the interface, and that the extent of the phenomenon depended strongly on an interplay between the equilibrium conditions and the diffusion rates in the system. In the present study, we extend this first analysis to also consider general three-component systems, and we then apply the arguments to qualitatively discuss some specific cases in lipid systems.

2. Three components. General considerations

For illustration purposes, consider the specific case of a bulk liquid with three components, including water, component A and lipid B. Here, A can be either a co-solvent, like urea or glycerol, a co-lipid, like cholesterol, or a surfactant. The liquid system has an interface to air with a given RH (defined as p/p^0, where p is the partial pressure of water vapour and p^0 is the saturation water vapour pressure), which corresponds to a chemical potential of water of $\Delta\mu(H_2O) = RT\ln(p/p^0)$. It is a common situation that the RH in air does not match $\mu(H_2O)$ in the liquid phase, meaning that, in general, the liquid and the air are not in equilibrium with respect to composition. Water is assumed to be the only volatile component, and conditions are chosen so that there is an evaporation of water at the interface. Given sufficient time, steady state conditions will be established across the interface. There is a constant evaporation rate and the interface will recede slowly due to the loss of material in the liquid phase. The concentration profile is then constant, if registered relative to the moving interface. One can, within reasonable approximation, also identify a profile in the chemical potentials of the different components across the interface. The water transport is driven by a gradient in the $\mu(H_2O)$. For a two-component system, the chemical potentials are directly interrelated through a Gibbs–Duhem equation, and thus there is only one independent diffusion process. With three components present, there is an additional degree of freedom. For a given profile in the chemical potential of water, it remains to determine the concentration and/or chemical potential profiles of the two other components.

ART ■ C2FD20079A

In the following discussions we will assume that the rate limiting transport process is the diffusion in the liquid phase close to the air–water interface. This implies that there is sufficient convection in the gas phase to ensure that the RH in the gas phase close to the interface is the same as in the bulk of the gas. It also implicitly assumes that heat conduction is sufficiently rapid to supply the energy of vaporization for the water. If not, then there will be a localized dip in the temperature in the interfacial region.[13] We further assume that the bulk solution is large enough so that even though there is some water evaporation, the bulk concentration can be assumed constant over the time frame considered. With these assumptions we know, in principle, the values of the $\mu(H_2O)$ in the bulk liquid and the $\mu(H_2O)$ at the interface. The central question is now: what phenomena we could expect to occur in the transition zone between bulk and surface?

Our approach in analysing the properties of the transition zone between the bulk and the air–liquid interface is to combine formalisms from irreversible thermodynamics, presented in detail in section 3, with the properties of equilibrium phase diagrams. Fig. 1 shows a schematic phase diagram of a model system. From the known bulk composition, we can mark one endpoint (X_{bulk}) of the concentration profile that develops at steady state. From the boundary condition at the interface, we know the $\mu(H_2O)$, although the ratio between component A and B is not known. This boundary condition is illustrated by the double dashed line, $\Phi(l \rightarrow g)$, in the phase diagram in Fig. 1, and some different possibilities for the concentration profiles that can develop at steady state are represented by dotted arrows. For some systems, the bulk composition and the compositions along the $\Phi(l \rightarrow g)$ line

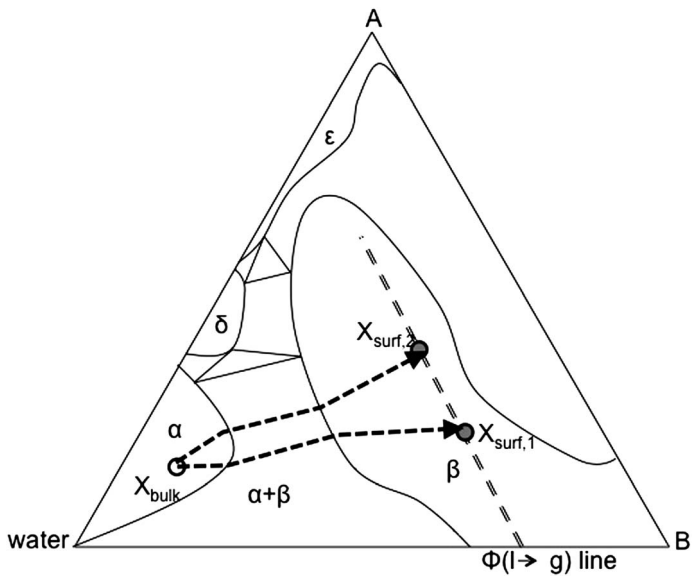

Fig. 1 Schematic illustration of a model phase diagram for a ternary system of component A, lipid B and water. The phase diagram contains four one-phase regions (phases α, β, δ, ε), two three-phase triangles and five 2-phase areas. The arrows illustrate two possible scenarios for the concentration profile that develops from the bulk solution towards the interface, with the head of the arrows pointing in the direction of the interface composition. The boundary conditions are given by the bulk composition, which defines the starting point X_{bulk} (open circle), and $\mu(H_2O)$ at the air–liquid interface (represented by a double dotted line, $\Phi(l \rightarrow g)$). The latter boundary condition is fulfilled for different ratios A/B, and the position of the endpoint (filled circles) depends on the diffusion coefficients of components A and B. In the figure, $X_{surf,1}$ corresponds to the situation where $D_A \gg D_B$, and $X_{surf,2}$ corresponds to the situation of ideal mixing and $D_A = D_B$.

ART ■ C2FD20079A

all are within the same one phase area (not shown). In such a case, there is a concentration gradient but no cause for large structural changes in the interfacial region under steady state conditions. For other systems, the $\Phi(l \rightarrow g)$ line (or parts of it) is located within another phase. For such a case, the surface composition may correspond to a different phase than found in the bulk, and then one can have the situation that a new phase actually forms at the interface. When applying these arguments to concrete examples, one can identify three main questions: (i) does one or more new phases appear in the interfacial region? (ii) If so, what are their compositions or composition profiles? (iii) How thick are the phases? To provide a basis for a more thorough analysis of these questions we now turn to a quantitative analysis of the diffusional transport.

3. Diffusion in a three-component system

3.1 Solvent evaporation and mass transport

In our earlier work,[10] we presented a hydrodynamic model for mass transport in a two-component system with water evaporation. The final result is that, at steady state, a non-volatile component fulfills the equation

$$J_{\mathrm{nv}}(z) = \dot{a} X_{\mathrm{nv}}(z) \tag{1}$$

if the coordinate, z, is chosen such that the air–liquid interface is stationary (Fig. 2). Here X_{nv} is the mass fraction and J_{nv} is the diffusional flux of the non-volatile component, respectively. $\dot{a}$ is the speed with which the interface moves with respect to the container. Actually, nothing in the derivation depends on the number of components, and eqn (1) is equally valid for any non-volatile component in an n-component system. We briefly reiterate the argument for completeness:

Our description is based upon separate equations of continuity for each component. Initially, we use a coordinate, z', centered on the container (Fig. 2). Assuming, for simplicity, equal densities of all components, we can formulate the equations of continuity in this coordinate system as[14]

$$\frac{\partial X_i}{\partial t} + \frac{\partial}{\partial z'}(v_i X_i) = 0 \tag{2}$$

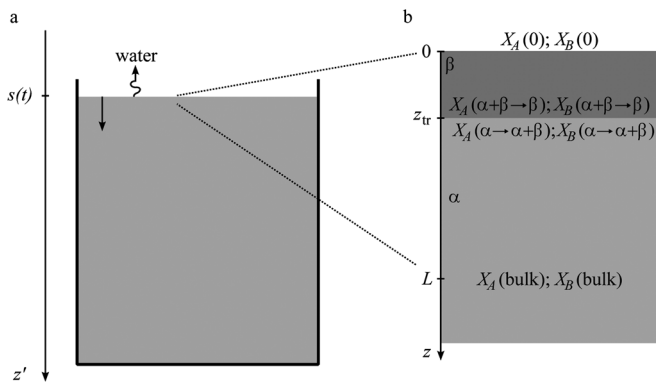

Fig. 2 Schematic of system and coordinate systems. (a) An aqueous solution exposed to the ambient atmosphere such that evaporation of water occurs. Due to the evaporation, the gas–liquid interface moves downwards. The z' coordinate system is defined with respect to the container. (b) Enlargement of the region close to the gas–liquid interface, showing the formation of a separate phase, β, on top of the bulk phase, α. The $z = z' - s(t)$ coordinate system employed here moves with the gas liquid interface. Within the 'unstirred layer' approximation, the concentration at the start, $z = L$, of the 'unstirred layer' is the same as in bulk.

where X_i and v_i is the mass fraction and local velocity of any (not just a non-volatile) component i, respectively. The total mass fraction flux of component i, v_iX_i, can be partitioned into two terms[14]

$$v_iX_i = vX_i + J_i. \tag{3}$$

The first term, vX_i, is due to transport of the fluid as a whole, which includes component i travelling along with the centre of mass velocity

$$v = \sum_i v_iX_i. \tag{4}$$

The centre of mass velocity is the quantity that enters the Navier–Stokes equation (or similar). We will have little to say about the centre of mass velocity because using the fact that the total mass fraction is unity, $\sum X_i = 1$, it follows from eqn (2) that v is independent of z'. Furthermore, since the centre of mass velocity necessarily vanishes at the bottom of the container, it follows that $v = 0$ everywhere. The second term, J_i, in eqn (3) is the diffusive flux, defined relative to the centre of mass velocity. Since the centre of mass velocity is zero, it follows from eqn (3) that the flux is completely diffusive, $J_i = v_iX_i$, and the problem simplifies considerably.

The evaporation of water causes the location of the air–liquid interface to move downwards. Consequently, steady-state conditions can be appropriately defined by using a coordinate system centered on the air–liquid interface, rather than on the container. We therefore switch to the coordinate system defined by

$$z = z' - s(t)$$

where $s(t)$ denotes the position of the air–liquid interface (see Fig. 2). At steady state, the interface moves with constant velocity, $\dot{a}$, and the mass fractions, X_i, (as a function of z) are independent of time. In principle, the steady-state will only occur for an infinitely large (in the z direction) container; in practice, an approximate steady-state occurs for a large enough container. The continuity equation, eqn (2) then reads

$$\frac{\partial}{\partial z}\left(X_i\left(v_i - \dot{s}\right)\right) = 0. \tag{5}$$

While a volatile component can escape through evaporation, the molecules of a non-volatile component at the interface are forced to move at the same velocity as the interface itself. For a non-volatile component we therefore find $v_{\mathrm{nv}}(z = 0) = \dot{a}$ for all t. Using this condition in an integration of eqn (5) and using the fact that the flux is completely diffusive, $J_{\mathrm{nv}} = v_{\mathrm{nv}}X_{\mathrm{nv}}$, then yields eqn (1).

3.2 Multi-component diffusion with evaporation

Eqn (1) is the governing equation for the concentration of a non-volatile solute. To go further, one must relate the diffusional fluxes to the local mass fractions. For a two-component system, Fick's first law, $J_i = -D\mathrm{d}X_i/\mathrm{d}z$, provides such a link. However, across a phase boundary there is often a gradient in concentration even at equilibrium, while no diffusional transport occurs under these conditions. In multi-phase systems, or inhomogeneous systems in general, Fick's first law therefore has to be used with care. Alternatively, one may utilise a generalised form of Fick's law[15]

$$J_i = -\frac{D_i}{RT}X_i\frac{d\mu_i}{dz} \tag{6}$$

wherein it is recognised that the driving force for the diffusional transport is the gradient in chemical potential, μ_i, rather than the gradient in concentration. The chemical potential varies smoothly over a phase boundary, and using this form of

ART ■ C2FD20079A

Fick's first law therefore does not predict any diffusional transport across an interface at equilibrium.

Insertion of eqn (6) into eqn (1) yields the equation

$$\frac{d\mu_{nv}}{dz} = -\dot{s}\frac{RT}{D_{nv}} \tag{7}$$

The simplicity of eqn (7) is, however, somewhat deceptive; if the diffusion coefficient, D_{nv}, is concentration dependent, then complications arise. Nevertheless, it is useful as a basis for qualitative discussions, as we demonstrate below.

Experimental phase diagrams are most often determined in terms of composition (as in Fig. 1), rather than chemical potentials. Consequently, we convert the general form of Fick's first law, eqn (6), into compositions[16]

$$J_i = -\frac{D_i}{RT}X_i\frac{d\mu_i}{dz} = -\frac{D_i}{RT}X_i\sum_j \frac{\partial\mu_i}{\partial X_j}\frac{dX_j}{dz}$$

from which we can find explicit expressions for the diffusion coefficient matrix; for our three-component system

$$\begin{aligned} J_A &= -\frac{D_A}{RT}X_A\frac{\partial\mu_A}{\partial X_A}\frac{dX_A}{dz} - \frac{D_A}{RT}X_A\frac{\partial\mu_A}{\partial X_B}\frac{dX_B}{dz} = -D_{AA}\frac{dX_A}{dz} - D_{AB}\frac{dX_B}{dz} \\ J_B &= -\frac{D_B}{RT}X_B\frac{\partial\mu_B}{\partial X_A}\frac{dX_A}{dz} - \frac{D_B}{RT}X_B\frac{\partial\mu_B}{\partial X_B}\frac{dX_B}{dz} = -D_{BA}\frac{dX_A}{dz} - D_{BB}\frac{dX_B}{dz}. \end{aligned} \tag{8}$$

where we have supressed the concentration-dependence of the diffusion coefficients, D_{ij}. Insertion into eqn (1) now yields

$$\begin{aligned} -D_{AA}\frac{dX_A}{dz} - D_{AB}\frac{dX_B}{dz} &= \dot{s}X_A \\ -D_{BA}\frac{dX_A}{dz} - D_{BB}\frac{dX_B}{dz} &= \dot{s}X_B. \end{aligned} \tag{9}$$

These are, supplemented by appropriate boundary conditions, the final governing equations of the problem.

3.3 Interfacial phase formation

In order to assess the potential formation of different phases at the air–liquid interface and their eventual compositions, we must relate the transport picture [eqn (9)] to the equilibrium phase behaviour (Fig. 1). This link is provided by the appropriate boundary conditions. As in our previous analysis of the two-component case,[10] we will analyse the situation in terms of an 'unstirred layer' picture. The reason for this is the recognition that in practice it is difficult to arrange an experimental setup wherein bulk flow is completely absent (for reasonable sample sizes). Within the 'unstirred layer' picture, we therefore assume that in the bulk of the solution mixing is efficient and the concentration uniform. Only in a thin layer of thickness L close to the air–liquid interface do the concentrations vary (see Fig. 2b). Consequently, the concentration at $z = L$ is uniquely determined by the bulk concentrations,

$$X_i(L) = X_i(\mathrm{bulk}). \tag{10}$$

A second boundary condition is provided by the $\mu(H_2O)$ in the gas phase. Writing the line of constant $\mu(H_2O)$; $\Phi(\mathrm{l} \rightarrow \mathrm{g})$ (Fig. 1) in terms of component A, we express this boundary condition as

$$X_B(0) = \Phi(\mathrm{l} \rightarrow \mathrm{g})(X_A(0)). \tag{11}$$

ART ■ C2FD20079A

The final link to the equilibrium phase behaviour is accomplished by considering the path in the phase diagram, *i.e.* by considering, say, X_B as a function of X_A. To this end, we solve for the gradients, dX_{nv}/dz in eqn (9) and divide one of the gradients with the other.[17] We then find

$$\frac{dX_B}{dX_A} = \frac{D_{AA}X_B - D_{BA}X_A}{D_{BB}X_A - D_{AB}X_B} \tag{12}$$

which describes the path in the phase diagram, neglecting the spatial dependence. The path begins at the point $X_A = X_A(\text{bulk})$; $X_B = X_B(\text{bulk})$ [eqn (10)] and ends somewhere on the line described by eqn (11). Two different schematic solutions are illustrated in Fig. 1. We again remind the reader that the diffusion coefficients, D_{ij}, are in general concentration dependent. However, eqn (12), contains no explicit spatial dependence.

In terms of chemical potentials, the corresponding procedure based upon eqn (7), rather than eqn (9), yields

$$\frac{d\mu_B}{d\mu_A} = \frac{D_A}{D_B}. \tag{13}$$

Regardless, how to find the path in the phase diagram is now, at least in principle, clear: integrate eqn (12) progressively (possibly numerically), and take note of whether any phase boundaries presents themselves along the path or not. If the path does not cross any phase boundary before reaching the line described by eqn (11), then the system is composed of a single phase. If, on the other hand, the path crosses a phase boundary, then it follows the tie line to the next phase, and the integration of eqn (12) continues from there. In principle one can, depending on the phase diagram, have the formation of several phases stacked on top of each other. We stress that, in general, the diffusion coefficients may be decisively different in the two phases, and the solution consequently depends on the diffusion coefficients in a rather intricate way.

With the path in the phase diagram known, the spatial dependence can be found by integration of eqn (9). We sketch the procedure for a system where just one phase, β, forms at the liquid–gas interface on top of a bulk phase α (Fig. 2b). From the path in the phase diagram, $X_B(X_A)$ is known in both phases. In particular, the concentrations on either side of the two phase region are known, and we denote these by $X_A(\alpha \rightarrow \alpha + \beta)$; $X_B(\alpha \rightarrow \alpha + \beta)$ and $X_A(\alpha + \beta \rightarrow \beta)$; $X_B(\alpha + \beta \rightarrow \beta)$, respectively (Fig. 2b). Furthermore, the concentrations at the gas–liquid interface, $X_A(0)$; $X_B(0)$, are also known. Solving for dX_A/dz in eqn (9) and integrating then yields

$$\int \frac{D_{AA}D_{BB} - D_{AB}D_{BA}}{D_{AB}X_B - D_{BB}X_A} dX_A = \dot{s} \int dz. \tag{14}$$

X_B is a known function of X_A, so the integral of the right-hand side is known. In either phase, eqn (14) can be used to find z as a function of X_A; inversion gives $X_A(z)$, and, since $X_B(X_A)$ is known, also $X_B(z)$.

In particular, the thickness, z_{tr}, of the film formed by β phase can be found from eqn (14) by integrating over both phases to yield

$$\dot{s}z_{tr} = \int_{X_A(0)}^{X_A(\alpha+\beta\longrightarrow\beta)} \frac{D^{\beta}_{AA}D^{\beta}_{BB} - D^{\beta}_{AB}D^{\beta}_{BA}}{D^{\beta}_{AB}X_B - D^{\beta}_{BB}X_A} dX_A \equiv I_{\beta}$$

$$\dot{s}(L - z_{tr}) = \int_{X_A(\alpha\longrightarrow\alpha+\beta)}^{X_A(\text{bulk})} \frac{D^{\alpha}_{AA}D^{\alpha}_{BB} - D^{\alpha}_{AB}D^{\alpha}_{BA}}{D^{\alpha}_{AB}X_B - D^{\alpha}_{BB}X_A} dX_A \equiv I_{\alpha}$$

and solving for z_{tr}

$$\frac{z_{tr}}{L} = \frac{I_\beta}{I_\alpha + I_\beta}. \quad (15)$$

Eqn (15) can be used to predict the existence, or not, of an interfacial phase, β, at the air–liquid interface for a system where the path in the phase diagram traverses one two-phase region. In order for the β phase to form, its thickness, z_{tr}, must be larger than a typical microscopical distance of the β phase. There is also a contribution due to surface free energy,[10] that we have neglected. The situation necessarily becomes more involved when the path in the phase diagram traverses several two-phase (or even three-phase) regions, though the basic formalism outlined here will provide a basis for extensions to such cases.

4. Two limiting cases

The formal analysis presented in the previous section can be used to quantitatively describe specific systems provided enough information on bulk properties is available. We performed such an analysis for a two-component system.[10] For three components the description easily becomes involved to the extent that one loses the overview. As a basis for further more qualitative discussions we consider two limiting cases of the general three-component situation. For the case where component A is a co-solvent it is a reasonable assumption that $D_A \gg D_B$. This implies that the concentration gradient is sustained through the slow diffusion of the lipid B and that there is a negligible gradient in the chemical potential of co-solvent A, μ(A). This follows immediately by an integration of eqn (13) for constant diffusion coefficients. In relation to the phase diagram of Fig. 1 the profile follows a path of constant μ(A). To locate such a path in the diagram one needs either a good thermodynamic model or a detailed experimental characterization of the system. The path from X_{bulk} to $X_{surf,1}$ in Fig. 1 shows a possible illustration of this case.

Another simple limiting case could be illustrated by the situation when component A is a lipid of similar character as component B. If one makes the (unrealistic) assumption that $D_A = D_B$ and that the two lipids mix ideally, this corresponds to the two-component case analysed before by us.[10] Since there is nothing in the transport model that makes a distinction between the two lipids, the path within the one-phase regions in the phase diagram should be along straight lines of constant lipid ratio, as illustrated by the path from X_{bulk} to $X_{surf,2}$ in Fig. 1. The analysis above confirms this; for ideal mixing, the cross diffusion coefficients in eqn (8) vanish and eqn (12) reads $dX_B/dX_A = X_B/X_A$ for equal diffusion coefficients, showing that the ratio remains constant.

Below we will discuss some illustrative cases where one could expect the formation of a transport-induced phase at the air–liquid interface. We will make use of the limiting cases as a basis for qualitative arguments. We will not apply the formalism of section 3 quantitatively, but rather use it as a conceptual basis for the discussions. The aim is more to inspire thinking about these non-equilibrium effects rather than to provide explanations of already existing experimental results. It is our hope that this approach is in line with the traditional spirit of the Faraday Discussions.

5. Water–octyl glucoside–phospholipid

Single-chain micelle-forming surfactants can be used to solubilize bilayer-forming lipids. The double chain lipids are taken up in the micelles, so they are present in an isotropic solution where they diffuse with the micellar aggregates. Conversely, the single chain surfactants enter, to some extent, the lipid bilayers, affecting their properties. Octyl glucoside (OG) is often used for solubilizing membrane lipids and membrane proteins. The phase equilibria in systems of OG and DMPC

(dimyristoyl phosphatidyl choline) have been determined by Keller *et al.*, using calorimetric methods.[18] In Fig. 3 we show a schematic phase diagram based on their results together with characterization of the binary OG–water and DMPC–water systems.[19–21] This can be used to illustrate the simplest scenario: there is an isotropic phase containing micelles above the CMC of the surfactant and these micelles can incorporate lipids. Outside the isotropic phase there is a large two-phase area, which on the far side ends in a one-phase area of a lamellar liquid crystalline L_α phase. At low water and low OG concentrations (in the lipid rich corner) there appears a L_β gel phase.

In the ternary isotropic one-phase solution, the $\mu(H_2O)$ is close to that of pure water, which corresponds to RH > 99%. When such a solution is exposed to a humid gas phase, a gradient in $\mu(H_2O)$ develops across the interface. Reasonable RH values in the gas phase are RH < 80%, and this corresponds to $\mu(H_2O)$ values way into the lamellar L_α phase or even into the L_β gel phase. If the composition of the bulk solution is close to the border to two-phase L_1–L_α solution one can, in principle; expect that a stack of bilayer should develop in the interfacial region for all concentrations of the surfactant under steady-state conditions. However, for surfactant concentrations below CMC, the lipid concentration in the solution is minute and, in practice, it takes a very long time for the lipids to reach the surface. For surfactant concentrations above the CMC, on the other hand, there is a pool of lipids in micellar aggregates, and the diffusion coefficient of the lipids is close to that of the surfactants in micelles. Thus, there exists a transport mechanism by which lipids can reach the interfacial region within reasonable time so that steady-state conditions can be established. In this limit one can consider the micelles as a pseudo-component. According to section 3, and also in line with the results in our previous studies of diffusion and interfacial phase behaviour in evaporating solutions,[10,16] the micelles are expected to adopt an exponential concentration profile in the bulk at steady-state. At the interface we expect the formation of a stack of bilayers. In line with

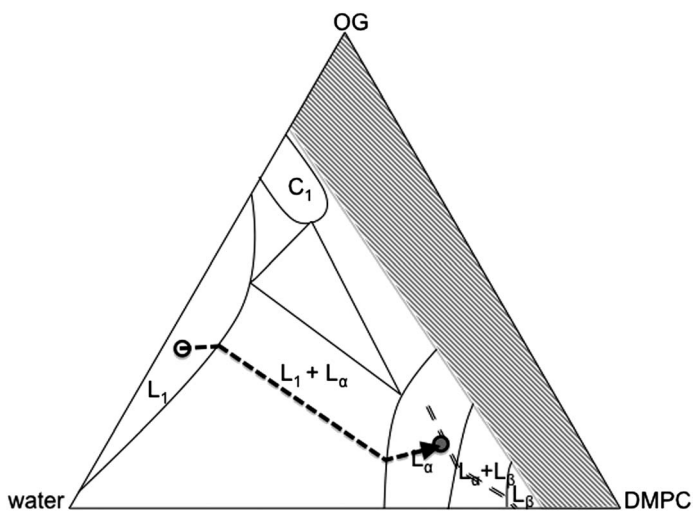

Fig. 3 Tentative phase diagram for the ternary system OG–DMPC–water (25 °C) based on combined data from previous studies.[18–21] The phase diagram contains four one-phase regions (isotropic micellar phase, L_1; liquid crystalline L_α lamellar phase; lamellar L_β gel phase; and bicontinuous cubic phase (C_1). The phase behaviour at low water contents is unknown (shaded). The double dashed line represent the conditions with constant $\mu(H_2O)$, in this case corresponding to around 70–80% RH at the air–liquid interface. The concentration profile for one situation is shown; from an isotropic L_1 bulk solution to an interfacial lamellar L_α phase is illustrated (dotted line with arrow).

ART ■ C2FD20079A

the pseudo-component picture the main composition change across this stack is reflected in a variation of the bilayer spacing, which causes a gradient in $\mu(H_2O)$. In Fig. 3 we have indicated a tentative composition path across the interfacial region at steady-state. Estimating the thickness of the bilayer stack requires a detailed model of the diffusional dynamics. We consider this to be a feasible task but it is outside the scope of the present paper.

6. Phospholipid vesicles in a mixed water–urea solvent

Phospholipids readily form bilayer structures also in mixed water–urea systems. In fact, urea is used in many natural situations[22–25] and in applications[26] to provide protection from conditions of high osmotic pressure, or equivalently, conditions of low $\mu(H_2O)$. We have, in another context, analysed in detail the thermodynamic lipid properties in mixed water–urea solvents. Fig. 4 reproduces a phase diagram of the system DMPC–water–urea at 27 °C. Let us now consider a system water–urea–DMPC, which has a surface exposed to air at RH = 70%. There is a gradient in the $\mu(H_2O)$ in the interfacial region. What structural effects can we expect to find in the interfacial region at steady state?

In Fig. 4, the line of constant $\mu(H_2O)$ corresponding to 70% RH is marked. For negligible urea contents the line goes through the L_β lipid gel phase. The addition of urea leads to a transition from the solid L_β phase to the liquid crystalline L_α phase. Let us first consider the binary water–DMPC system. At steady-state (if it can be established) we expect that the interfacial region consists of first a monolayer then a few bilayers of L_β character and then some L_α bilayers facing the bulk water. In

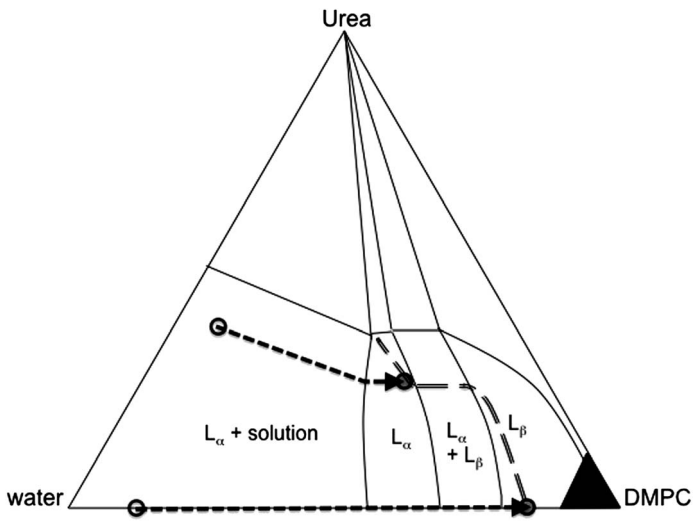

Fig. 4 Schematic phase diagram for the ternary system water–urea–DMPC (27 °C) based on combined data from previous studies.[27,28] The L_α and L_β gel phases are formed both in pure water and in an aqueous phase that also contain urea. The double dashed line represent the conditions with constant $\mu(H_2O)$, in this case corresponding to around 70% RH at the air–liquid interface. At low urea contents, this $\mu(H_2O)$ corresponds to an L_β gel phase, while at higher urea contents, L_α is the stable phase at the same $\mu(H_2O)$. Two different scenarios are shown (dotted lines with arrows), in both cases the bulk phase is an isotropic micellar solution. In the binary DMPC–water system, the concentration profile goes from an isotropic L_1 solution in bulk to an interfacial film that contain a lamellar L_α phase in the layer of the film that faces the bulk solution, and a L_β gel phase in the part of the film that is exposed to air with the given RH. In the presence of urea, the L_α phase is stable at all RH, and the interfacial film is a L_α phase.

ART ■ C2FD20079A

the presence of urea the composition profile in the interfacial region will depend on diffusion properties as discussed in section 3. For sufficiently high urea content the L_β part of the interfacial region no longer occurs. One then only finds a stack of L_α bilayers at the interface, with, relatively seen, larger interbilayer separations. In Fig. 4 we show estimated steady-state concentration paths across the interfacial region in the absence or presence of urea. The fact that there are no bilayers in the gel state when urea is present can be seen as yet another illustration of the physiological effect of urea to maintain a liquid crystalline structure under dry conditions.[27,28] Such an effect could be of relevance for the liquid film in the eyes.[9]

7. Phospholipid vesicles in a mixed D_2O–H_2O system

Consider a system where unilamellar phospholipid vesicles have been prepared in pure H_2O. Assume that the lipid bilayer has a density slightly above 1.0×10^3 kg m^{-3}. In a quiescent liquid the vesicles will settle to the bottom of the container. However, this is a slow process and, in practice, there is always some convection that keeps the vesicle concentration rather homogeneous in the system. Now, the liquid sample with an open air–water surface is placed in a big container where the RH is substantially less than 100%. For the case when the water vapour is made from D_2O we expect some special effects since a mass density gradient develops across the interface. What structures can form at the surface at steady state? Irrespective of the detailed conditions, a lipid monolayer is present at the surface. When the liquid sample is exposed to the D_2O atmosphere, there will be a condensation and diffusional transport of heavy water into the liquid, and a somewhat larger evaporation and diffusional transport of ordinary H_2O into the gas phase. Hence, in the aqueous system the interfacial region will have a mixed composition, resulting in a density gradient. Vesicles in the liquid can slowly float towards the monolayer at the surface. Is there a possibility that vesicle fusion can occur in this environment?

There is a gradient in the water (D_2O + H_2O) chemical potential across the interface. The thickness of this region is determined by the competition of different diffusion processes. It is important to realize that a RH of 60% corresponds to a large osmotic pressure of 70 MPa at 25 °C. Thus, surface vesicles are pushed towards the monolayer with substantial force, and the tendency for fusion will be strongly increased. We are not in the position to claim that fusion will occur, but it is certainly a possibility. Assuming that the vesicles are labile enough for fusion to occur, a lamellar system will gradually develop at the interface. With an unstirred layer, there is no convection, and close to the surface a steady state will develop as previously described.[10] The interfacial phase will here consist of a number of bilayers separated by a water layer with varying D_2O–H_2O ratio and varying thickness. The envisaged formation process is shown in Fig. 5.

8. Water–bile salt–phospholipid

In higher animals the digestion of lipids proceeds through a solubilisation process involving bile. The main components of bile are bile salts, phospholipids and cholesterol. The aggregation properties of the components of bile have been extensively studied, and in particular, there are many studies of ternary systems composed of water–bile salt–phospholipid.[29–32] The emphasis of these investigations has been the relation between lamellar aggregates, micelles of different shapes and the formation of hexagonal and cubic liquid crystalline phases. Fig. 6 shows the phase diagram of the system water–sodium cholate–lecithin. In addition to the micellar solution there are three different liquid crystalline phases, including a lamellar phase (L_α), a normal hexagonal phase (H_1) and a bicontinuous cubic phase (C_1).

If an isotropic micellar solution is exposed to an interface with air of RH $\approx$ 60%, we can expect a more complex pattern of structures than discussed in the previous

ART ■ C2FD20079A

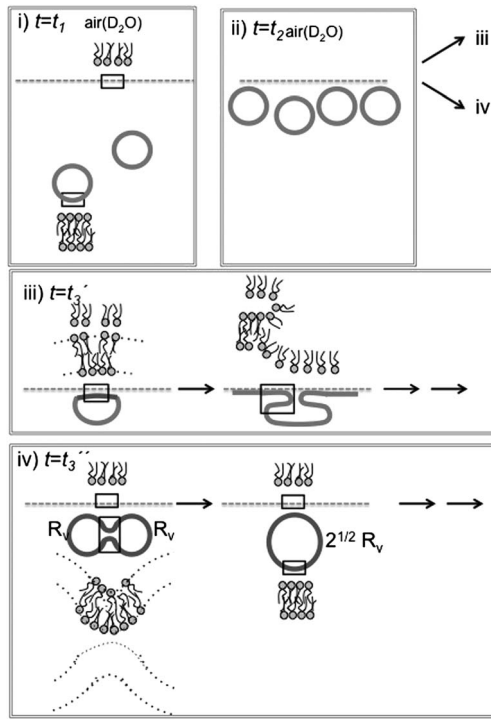

Fig. 5 Schematic illustration of a solution of unilamellar phospholipid vesicles in pure H_2O that is placed in an atmosphere with water vapour made from D_2O (RH $\ll$ 100%). In the aqueous system, the interfacial region will have a mixed composition of D_2O and H_2O, resulting in a density gradient. The figure illustrates some possible scenarios for the evolution in the interfacial regime at different times. (i) $t = t_1$: Vesicles are present in the solution, and a lipid monolayer is present at the air–liquid interface. (ii) $t = t_2$: Due to the density gradient, vesicles in the liquid slowly float towards the monolayer at the surface. At the interface, the vesicles are exposed to relatively high osmotic pressure (set by the RH in air), which can lead to vesicle fusion. Two possible scenarios are envisioned (iii and iv): (iii) $t = t_3'$: The surface vesicles are pushed towards the monolayer, leading to deformation and eventually fusion, and formation of oriented multilayer lipid structures. (iv) $t = t_3''$: Fusion of vesicles in the interfacial layer, and formation of larger vesicles.

cases. In the isotropic solution, both phospholipids and cholate diffuse with the micelles and these two components have effective diffusion constants of the same order of magnitude. Due to the solubilisation in micelles, the transport is fast enough so that steady–state conditions can be reached within reasonable times. Due to the presence of the charged cholate molecules, there is a long-range double layer repulsion between aggregates. Thus, a gradient in the $\mu(H_2O)$ can develop gradually as the concentration of the other components increases on approaching the surface. This effect will tend to make the interfacial layer thicker than for the non-charged systems.

In Fig. 6 we have marked three tentative concentration profiles of the interfacial region, and the interfacial films that could form in these systems are schematically illustrated in Fig. 7. For case (i), the bulk solution has a low bile salt to phospholipid ratio. Then, we expect that the concentration profile crosses the boundary to the L_1–L_α phase coexistence region. In this case, the interfacial region consists of lamellar structures where the interbilayer separations decrease markedly towards the surface. For case (ii) with a higher cholate to phospholipid ratio, the concentration profile goes across the boundary of coexistence L_1–H_1 phase. Thus, in the interfacial region

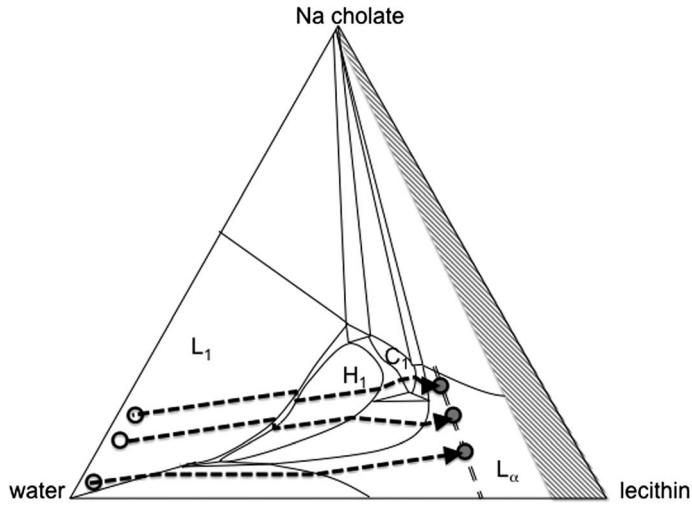

Fig. 6 Schematic phase diagram for the ternary system Na cholate–lecithin–water (25 °C).[29] The phase diagram contains four one-phase regions (isotropic micellar phase, L_1; liquid crystalline L_α lamellar phase; normal hexagonal phase (H_1) and bicontinuous cubic phase (C_1)). The low water content region remains uncharacterized (shaded). The double dashed line represents $\mu(H_2O)$ that corresponds to around 60% RH at the air–liquid interface. Three different scenarios are indicated (dotted line with arrows), and the tentative structures in the interfacial films for these three cases are illustrated in Fig. 7. For all three cases, the bulk is an iostropic micellar L_1 solution, while the cholate–lecithin ratio differs between the three cases: (i) at low cholate–lecithin ratio, one goes from L_1 solution in bulk to an interfacial lamellar L_α phase. (ii) At intermediate cholate–lecithin ratio, one goes from L_1 solution in bulk to an interfacial phase that form an H_1 structure in the lower layers, and a lamellar L_α phase in the part of the film that is exposed to air with the given RH. (iii) At higher cholate–lecithin ratio, one goes from L_1 solution in bulk to an interfacial phase that forms an H_1 structure in the lower layers, followed by a bicontinuous cubic phase, C_1, and finally a lamellar L_α phase in the part of the film that is exposed to air.

the isotropic solution will be exposed to a hexagonal phase. Further into this region, the hexagonal phase loses water until a concentrated lamellar phase appears. In the third case (iii), the bulk concentration is even richer in cholate relative to the phospholipid. For this case, it is conceivable that first a hexagonal phase forms, as in case II.

When the $\mu(H_2O)$ decreases further, a bicontinuous cubic phase can form, and this, in turn, is followed by a lamellar phase at even $\mu(H_2O)$ (water contents).

9. Discussion

An interface between an aqueous solution and air of ambient RH is a non-equilibrium system, where there is an evaporation of water. As a consequence of this, concentration gradients will evolve in the interfacial region. Above we have analysed the case where there are two components in the solution in addition to the water. In section 3 the formal transport equations were established. In the following sections, the same problem has been analysed in more qualitative terms when applied to some specific systems. The analysis is built on combining the descriptions of diffusional processes and equilibrium phase behaviour, and it illustrates a useful application of existing phase diagrams. The most important conclusion from the analysis is that, having non-equilibrium conditions in a system with self-assembly aggregation, gives rise to a potentially rich behaviour in the interfacial region. There are experimental observations of such phenomena,[4–8] but very few systematic investigations

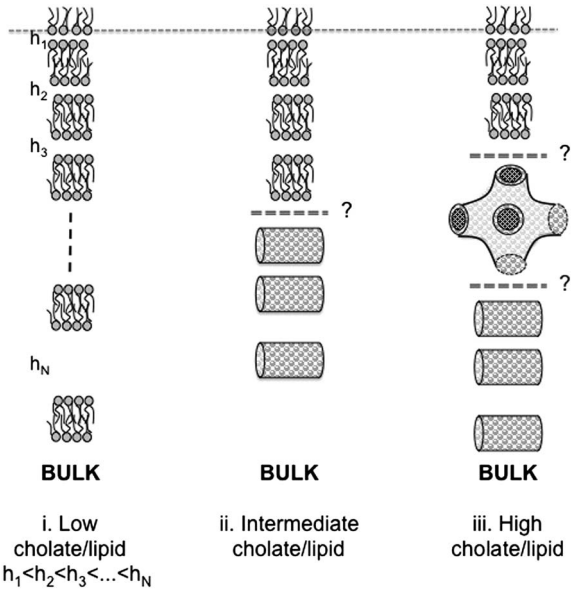

Fig. 7 Schematic illustrations of possible sequences of structure in interfacial films that may form in ternary systems composed of Na cholate–lecithin–water. Three different scenarios that correspond to the cases in Fig. 6 are shown: (i) for low cholate–lecithin ratio, the interfacial film consists of a lamellar phase. The interlamellar distance varies with the position within the film due to the gradient in $\mu(H_2O)$, and the most swollen structure is found in the lower layers of the film. (ii) At intermediate cholate–lecithin ratio, a transition from an H_1 phase to a lamellar L_α phase takes place within the film as $\mu(H_2O)$ decreases when approaching the surface. (iii) At higher cholate–lecithin ratio, a transition from an H_1 phase to a bicontinuous cubic phase, C1, and then to an L_α phase can occur in the $\mu(H_2O)$ gradient.

have so far been performed. Apart from the fundamental aspects we see several applications of the concept for lipid systems. Our starting point has been efforts to understand how (human) skin responds to changes in the RH of the air. We have demonstrated both that the transport properties of the skin depend strongly on RH,[1] and also demonstrated that this is correlated with structural changes on the molecular level.[2,33–35] Another physiological case where these effects can be relevant is for the liquid film of the cornea.[9]

In section 5 and 7, we discussed two different possibilities for formation of oriented multilamellar structures at the air–water interface, either by the use of micelles as transporters of insoluble lipids, or due to the interfacial density gradient that can occur if the lipid solution is exposed to an atmosphere with D_2O. One area of application of this is the preparation of thin ordered lamellar structures, where also other components can be incorporated. It should be possible to form a thin film at an interface and then transfer it to a solid substrate. By using a polymerisable lipid, we might also be able produce a film that is robust enough to be removed without solid substrate. Such thin films could offer interesting material properties, and could also provide new model membrane systems. The formation of oriented interfacial structures can be compared with established methods for depositing bilayers at solid surfaces, which rely on vesicle fusion near the interface[39] or deposition from mixed micelles.[38] These methods rely on different mechanisms than discussed in this paper, although slightly related.

In Fig. 7, the positions that denote the interfaces between the different liquid crystalline parts are marked with question marks. This signifies another interesting and open question that is related to how the interface between two liquid crystalline

phases looks like. One application of interfacial films in systems with complex phase behaviour would be to create model systems for interfaces between different structures, in accordance with the discussion in section 8. This can also have direct applications in, *e.g.*, biomembrane systems. The occurrence of continuous foldings and unfoldings between cubic and lamellar structures has been demonstrated in some biological membranes.[36,37] Such cycles have also been suggested as a possible mechanism for the transition from the lamellar bodies of stratum granulosum to the planar bilayers of the extracellular lipids of stratum corneum.[40] We are currently pursuing some of the possible applications of interfacial films.

Acknowledgements

Karen Edler and Tahereh Mokhtari are acknowledged for fruitful discussions. The authors gratefully acknowledge financial support from the Swedish Research Council (Vetenskapsrådet) both through regular grants and a Linneaus programme. E.S. acknowledges The Swedish Foundation for Strategic Research (Stiftelsen för Strategisk Forskning) for financial support. C.Å. acknowledges financial support from Science Foundation Ireland under Grant No. [09/RFP/MTR2425] and the European Union Seventh Framework Programme project NanoTransKinetics under grant agreement no. 266737.

Notes and references

1 S. Björklund, J. Engblom, K. Thuresson and E. Sparr, *J. Controlled Release*, 2010, **143**, 191.
2 E. Sparr, C. Åberg,, P. Nilsson, and H. Wennerström,, *Soft Matter*, 2009, **5**, 3225.
3 C. Åberg, E. Sparr, M. Larsson and H. Wennerström, *J. R. Soc. Interface*, 2010, **7**, 1403.
4 B. M. D. O'Driscoll, E. A. Nickels and K. J. Edler, *Chem. Commun.*, 2007, 1068.
5 K. J. Edler, A. Goldar, T. Brennan and S. J. Roser, *Chem. Commun.*, 2003, 1724.
6 G. Cevc, W. Fenzl and L. Sigl, *Science*, 1990, **249**, 1161.
7 Z. X. Li, J. R. Lu, R. K. Thomas and J. Penfold,, *Faraday Discuss.*, 1996, **104**, 127.
8 Z. X. Li, A. Weller, R. K. Thomas, A. R. Rennie, J. R. P. Webster, J. Penfold, R. K. Heenan and R. Cubitt, *J. Phys. Chem. B*, 1999, **103**, 10800.
9 M. Mitra, G. J. Menon, A. Casini, S. Hamada, D. Adams, C. Ricketts, E. T. Fuller and J. R. Fuller, *Eye*, 2005, **19**, 657.
10 C. Åberg, E. Sparr, K. J. Edler and H. Wennerström, *Langmuir*, 2009, **25**, 12177.
11 A. Khan, B. Jönsson and H. Wennerström, *J. Phys. Chem.*, 1985, **89**, 5180.
12 B. Jönsson and H. Wennerström, *J. Phys. Chem.*, 1987, **91**, 338.
13 H. K. Cammenga, D. Schreiber and B. E. Rudolph, *J. Colloid Interface Sci.*, 1983, **92**, 181.
14 S. R. de Groot and P. Mazur, *Non-Equilibrium Thermodynamics*, Dover Publications Inc.: New York, 1984.
15 D. F. Evans and H. Wennerström, *The Colloidal Domain, where Physics, Chemistry and Biology meet*, ch. 6, VCH Publishers, Inc.: New York, 1999.
16 A. Kabalnov and H. Wennerström, *Soft Matter*, 2009, **5**, 4712.
17 C. Åberg and H. Wennerstrom, *Phys. Chem. Chem. Phys.*, 2009, **11**, 9075.
18 M. Keller, A. Kerth and A. Blume, *Biochim. Biophys. Acta, Biomembr.*, 1997, **1326**, 178.
19 V. Kocherbitov, O. Soderman and L. Wadso, *J. Phys. Chem. B*, 2002, **106**, 2910.
20 M. J. Janiak, D. M. Small and G. G. Shipley, *J. Biol. Chem.*, 1979, **254**, 6068.
21 N. Markova, E. Sparr, L. Wadsö and H. Wennerström, *J. Phys. Chem. B*, 2000, **104**, 8053.
22 K. N. Barton, M. M. Buhr and J. S. Ballantyne, *Am. J. Physiol.-Regul. Integr. Comp. Physiol.*, 1999, **276**, R397.
23 D. F. Perlman and L. Goldstein, Nitrogen metabolism, in *Physiology of Elasmobranch Fishes*, ed. T. J. Shuttleworth, Springer-Verlag: New York, 1989, p. 253.
24 A. V. Rawlings, I. R. Scott, C. R. Harding and P. A. Bowser, *J. Invest. Dermatol.*, 1994, **103**, 731.
25 N. Nakagawa, S. Sakai, M. Matsumoto, K. Yamada, M. Nagano, T. Yuki, Y. Sumida and H. Uchiwa, *J. Invest. Dermatol.*, 2004, **122**, 755.
26 M. Lodén, *J. Eur. Acad. Dermatol. Venereol.*, 2005, **19**, 672.
27 F. O. Costa-Balogh, H. Wennerström, L. Wadsö and E. Sparr, *J. Phys. Chem. B*, 2006, **110**, 23845.
28 A. Nowacka, S. Douzan, D. Topgaard, L., W and E. Sparr,, *Soft Matter*, 2012, **8**, 1482.

29 D. M. Small, M. C. Bourges and D. G. Dervichi, *Biochim. Biophys. Acta, Lipids Lipid Metab.*, 1966, **125**, 563.
30 J. Ulmius, G. Lindblom, H. Wennerström, L. B. A. Johansson, K. Fontell, O. Söderman and G. Arvidsson, *Biochemistry*, 1982, **21**, 1553.
31 S. U. Egelhaaf and P. Schurtenberger, *J. Phys. Chem.*, 1994, **98**, 8560.
32 A. de la Maza and J. L. Parra,, *Colloids Surf., A*, 1997, **127**, 125.
33 S Björklund, A Nowacka, J Bouwstra, E Sparr, D Topgaard, Manuscript, submitted.
34 C. Silva, D. Topgaard, V. Kocherbitov, S. Jjs, A. Pais, and E. Sparr, *Biochim. Biophys. Acta, Biomembr.*, 2007, **1768**, 2647.
35 E. Sparr and H. Wennerström, *Biophys. J.*, 2001, **81**, 1014.
36 T. Landh, *FEBS Lett.*, 1995, **369**, 13.
37 Z. A. Almsherqi, T. Landh, S. D. Kohlwein and Y. R. Deng, Cubic Membranes: The Missing Dimension Of Cell Membrane Organization, in *International Review of Cell and Molecular Biology*, 2009, vol. 274, p. 275.
38 H. P. Vacklin, F. Tiberg and R. K. Thomas, *Biochim. Biophys. Acta, Biomembr.*, 2005, **1668**, 17.
39 E. Reimhult, F. Höök and B. Kasemo, *J. Chem. Phys.*, 2002, **117**, 7401.
40 L. Norlén, *J. Invest. Dermatol.*, 2001, **117**, 823.

